NINETEENTH EUROPEAN ROTORCRAFT FORUM

Paper No. G1

WIND TUNNEL TESTING OF A EUROFAR TILT ROTOR AEROELASTIC STABILITY MODEL

D A C JESSOP, P T W JUGGINS
WESTLAND HELICOPTERS LIMITED

September 14-16, 1993
CERNOBBIO (Como)
ITALY

ASSOCIAZIONE INDUSTRIE AEROSPAZIALI
ASSOCIAZIONE ITALIANA DI AERONAUTICA ED ASTRONAUTICA

WIND TUNNEL TESTING OF A EUROFAR TILT ROTOR AEROELASTIC STABILITY MODEL

D A C JESSOP, P T W JUGGINS
WESTLAND HELICOPTERS LIMITED

ABSTRACT

The EUROFAR Phase One study into tilt rotor aircraft (a EUREKA Project) included the design and testing of a 1/6 scale, half tip speed model of a rotor, nacelle and wing for aeroelastic (whirl flutter) stability investigations.

The model was of modular construction to enable the stability test and an additional aerodynamic test (not reported here) to be performed. The design was derived from the EUROFAR baseline vehicle data.

The construction of the aeroelastic stability model is explained together with the substantiation of specific model components. Various stages of commissioning were carried out prior to wind tunnel testing and a brief description of these is given.

The model was tested at the UTRC wind tunnel at Hartford, Connecticut USA in January 1993. The report details the installation of the model and describes the test procedure to explore the stability boundary for different model parameters. Results included show that the stability boundary limits in cruise configuration were successfully defined. A description of testing carried out through the conversion regime to establish loads and trim data is also included, together with initial results.

The stability and loads measurements made form the basis for validation of prediction methods used in the design of the EUROFAR tilt rotor aircraft, contributing to the EUROFAR tilt rotor technical database.

1. INTRODUCTION

The EUROFAR Phase One study into tilt rotor aircraft included the design and testing of a dynamically-scaled model of a rotor, nacelle and wing for aeroelastic (whirl flutter) stability in cruise flight, and as a secondary objective, for loads and trim data, particularly in the conversion corridor between hover and cruise flight.

The model was to provide data for validation of prediction methods for aeroelastic stability and loads. It would sufficiently represent the full scale aircraft to provide an assessment of flight boundaries, in terms of stability margins and provide load data for extrapolation to full scale. It would also provide stability and loads data for future use, in the EUROFAR tilt rotor database. As the third in a series of wind tunnel tests for EUROFAR Phase One (refs 1 and 2), the model is designated as Model 3.

The model was designed in modular form as a collaboration between Westland Helicopters Limited (WHL), of the UK and Sikorsky Aircraft of the USA. This enabled Sikorsky to perform aerodynamic testing of a variable diameter rotor (VDTR) (not reported here), using common components with the Model 3 test.

Some compromise in the true representation of the full scale aircraft was introduced by physical constraints (particularly to mass scaling) and by commonality with the VDTR test. In particular, a 3-blade rather than 4-blade configuration was adopted, as was half-tip-speed velocity scaling. Other parameters conformed to 1/6 scale dynamic scaling, with notable exceptions of rotor head and nacelle masses, and wing stiffnesses.

Model 3 was tested in the United Technologies Research Centre (UTRC) wind tunnel, Hartford, Connecticut USA, in January 1993, using a Sikorsky test crew with two WHL participants. Prior to the test, component qualification tests were performed at WHL, as was a rotor head commissioning test. Commissioning tests of the model were performed in the Sikorsky hover test facility and at the UTRC wind tunnel.

The aeroelastic stability test successfully defined the stability boundaries for 5 different rotor configurations, with frequencies and damping measured through the wind speed range for the wing modes and blade lead-lag mode. Loads and trim data in conversion were successfully obtained, defining a high speed boundary of the conversion corridor.

2. GENERAL MODEL DESCRIPTION

The aeroelastic stability model (Model 3) is a $^1/_6$ scale Reduced (½) Tip Speed model (Figure 1). The EUROFAR baseline vehicle, which is a 13.6T 30 PAX civil aircraft, was used to define the model parameters. The major dimensions are given in the table below.

Rotor Diameter	½ Wing Span	Wing Chord	Wing Thickness
1.868 m	1.225 m	0.4 m	23%

Due to the large differences between scaled and achievable values of rotor head mass, nacelle mass and nacelle inertia, scaling laws of the wing dynamics were relaxed. If scaled wing frequencies were retained, the stability margins were predicted to be excessive, due to the effect of the large inertias. Studies showed that retaining wing stiffnesses of approximately the same order as the scaled stiffnesses, rather than scaling frequencies, would give stability margins comparable with full scale.

Within these guidelines, a qualitative approach to wing stiffness scaling was adopted. Efforts were made to place fundamental wing bending and torsion frequencies close together, in order to ensure a system with a significant amount of coupling between nacelle degrees of freedom, which was a characteristic of the baseline aircraft. Different wing configurations were sought by varying the tilting mechanism stiffness.

As a consequence of the wing scaling philosophy, the relationship between rotor frequencies (which remained scaled) and wing frequencies was very different from full scale. The use of 3 blades, rather than 4 as in the full-scale aircraft, did not change the cyclic and collective mode dynamics, which are the contributors to whirl-flutter. The model was to provide validation data for prediction methods, rather than stability data for the aircraft, whilst retaining as many features of the aircraft as possible. As a result of this

strategy, efforts were also made in the wing scaling to ensure that at least one configuration of the model was unstable in cruise within the tunnel test speed range, since the most accurate and meaningful validation data would be obtained close to the stability boundary.

The model was of a port wing/nacelle assembly mounted vertically in the wind tunnel. The rotor was driven from a hydraulic motor mounted at the base of the wing and rotated clockwise when viewed from the front. Excitation of the model was by use of the swashplate hydraulic actuators and could be excited by collective, longitudinal cyclic, and lateral cyclic pitch inputs over a frequency range of 3-40 Hz.

Blade. The blades were highly twisted, with spanwise variation of thickness and chord. The blade sections used in the model were standard NACA profiles rather than the EUROFAR baseline aircraft defined profiles, and were selected to give the same scaled performance in the cruise as the aircraft proprotor. The rotor blades were fabricated in composite material and featured a steel flexure between the pitch bearing housing and 30% blade rotor radius. To meet the mass distribution whilst not exceeding the stiffness requirements, the spar core was made of cast polyurethane. Also the trailing edge skin was a single layer of film adhesive over a foam core. The blade profile extended inboard beyond the flexure attachment point as a fairing. Two blades had strain gauges in-built during manufacture to monitor flap, lag and torsion. All flexures were strain gauged.

Rotor Head. The rotor head (Figure 2) was a three-bladed gimbal configuration. To alleviate steady loads in the blades and hub there was 2.5° precone and 5.75 mm torque offset. The rotor also had 29 mm of undersling. An elastomeric spherical bearing was used for the central gimbal bearing. Homokinetic torque transfer was achieved using a laminated metal bellows. A safety drive was incorporated in the rotor head in case of bellows failure. The blades were attached to the rotor head via pitch bearing housings containing angular contact bearings. Blade pitch arms were manufactured having an effective blade pitch-flap coupling (δ_3) of 0°, +20° and -20°, 0° being the datum configuration. Blade pitch information was obtained directly from the blade pitch housing using a rotary potentiometer. Gimbal tilt was measured at the three blade positions using rotary potentiometers mounted above the bellows.

Nacelle. (Figures 3 and 4) The aircraft nacelle information was used as a guide to define an overall fairing envelope for the model. (The baseline vehicle has a stationary engine in-line with the tilting nacelle). Deviations from the aircraft profile were necessary to simplify the design and accommodate all the hardware necessary. The fixed nacelle structure consisted of an inner and outer side plate, and forward and rear arch. The forward arch also served as a hydraulic manifold. Oilite bearings were fitted to the side plates. The transmission, a right angle gearbox, was located in these via trunnions on each side of the main body, allowing the forward part of the nacelle to tilt. A potentiometer assembly gave nacelle tilt angle. A remotely operated tilt mechanism was fitted consisting of a hydraulic actuator mounted to the fixed nacelle via a torsion bar assembly. Changes in tilt actuator stiffness were achieved by changing the torsion bar. A six degree of freedom strain gauged balance was located between the transmission output shaft and rotor head base. Instrumentation wiring for the balance, rotor head, blades and push rods passed through the rotor shaft to a slip ring mounted on the rear of the transmission housing. The swashplate assembly was mounted to the transmission

output shaft via a spherical bearing. Push rods connecting the upper rotating swashplate to the pitch arms were strain gauged to provide control load data. The rotating scissors was attached to the shaft by means of a friction clamp to accommodate the different δ_3 settings. Flexible hydraulic pipes were used to connect both the swashplate actuators and tilt actuator to the manifold.

Wing. The structural element of the wing was a rectangular section epoxy thermoset composite box spar made primarily of unidirectional carbon fibre laid along its length. Two plies of unidirectional glass at +45°/-45° were laid on the inner and outer surface to improve the structural integrity. Stiffness measurements were made on a test specimen to ensure the section properties were acceptable. To provide an attachment between the wing tip and nacelle a steel bracket with plug was bonded to the inside of the spar. A bolted joint was used at the root end. Foam blocks were machined to the wing profile and bonded to the spar. Woven glass was bonded to the outer surface to provide a damage tolerant surface. Chordwise cuts through the outer skin and foam were made at intervals along the wing to minimise their stiffening effect. (Tape was used to cover the slits in the leading edge during wind tunnel testing). Flaps were not included on the model wing. The wing housed the drive shaft connecting the drive motor to the nacelle transmission. The drive shaft had standard Hooke's joints at each end and was telescopic to accommodate any length changes during wing deflections. Analysis had shown the whirl speed was above the maximum running speed. The wing also housed both the hydraulic pipes and electrical wiring. A cut-out was made in the wing upper foam by the nacelle to house accelerometers to measure beamwise and chordwise accelerations.

Test Stand. A steel tube supporting the drive motor was mounted to the wind tunnel balance. An encoder driven from the motor shaft gave both speed and relative position. An elliptical fairing placed around the test stand assembly was bolted to the floor of the wind tunnel and all electrical wiring and hydraulic pipes contained within this. The reflection plane (simulating the full-span aerodynamic environment) was connected by struts to the elliptical fairing and also served as a working platform.

3. SUBSTANTIATION OF MODEL

Because of the nature of the wind tunnel test the model was to be subjected to a significant fatigue environment. In addition the test programme only allowed for 120 hours of tunnel occupancy, this to be achieved in a single entry into the wind tunnel. The complexity of the model and the hazardous nature of the tests made it imperative that the strength and performance of the model be established, both by calculation and by testing of representative components.

Predictions were made to define loads distributions for representative static and endurance cases. The endurance cases were chosen to represent severe conditions at the edge of the conversion and cruise envelopes. These were used to define endurance loads for the hub, flexure and blades. The proposed test programme was also used to define a gimbal flapping spectrum for the elastomeric gimbal bearing. Using a 5th power combination law, the equivalent continuous flapping angle was calculated as 2.97 degrees.

Blade. The fatigue strength of the blades was confirmed by comparison with previous fatigue tests carried out on sections of blades similar in construction and size used in other model tests.

Blade Flexure. A fatigue test was carried out on the blade flexure with a representative bending moment distribution along its length. This together with the blade substantiation enabled the test monitor limits for blades to be set.

Bellows. Because of the design of the rotor head the bellows was to be subjected to large angular displacements (cocking) about one end. It was also required to transmit torque up to 68 Nm. The bellows was tested under both conditions simultaneously. The bellows initially proposed for the rotor head was found to have a static torsional instability well below the torsion design limit. A number of configurations were tested to overcome this problem leading to the final design. This was tested to 108 Nm (the rig limit) with no instability. Testing was carried out at various cocking angles to establish an endurance curve giving a limit for the bellows of 3.11° for infinite life.

Pitch Bearings. Micro-welding of ball bearings due to small oscillatory movements had been encountered on a previous model rotor at WHL. To examine the possibility of this occurring with the proposed design steady centrifugal and lag forces were applied to a pair of pitch bearing assemblies by attaching a large weight to the bearing housing and off-setting the bearing spindle. A small amount of oscillatory motion was applied via the swashplate. Micro-welding occurred but was found to be dependent on the grease used, and suitable lubrication eliminated it.

Rotor Hub Spindle. A pitch bearing assembly and test spindle were manufactured prior to final design of the rotor head components to clarify certain design issues, ie. ease of assembly, torque tightening values, etc. The model rotor hub was manufactured from stock bar but due to geometric constraints, the bearing spindles had to be machined across the grain. Although fatigue data were available there was a concern over the likely scatter. Also the bearings may have induced fretting, reducing the fatigue life. The test spindle was also machined across the grain. Additional tests were carried out using the blade flexure attached to the pitch bearing assembly and test spindle. Subsequent examination showed no signs of fretting on the spindle. This enabled the monitor limits for the blades to be confirmed.

Gimbal Potentiometer Assembly. The gimbal measurement assembly was a novel design utilising thin nylon line tensioned against a spring/pulley attached to a potentiometer. The major concerns were the effect of centrifugal force on the nylon line, high angular accelerations likely to be experienced by the potentiometer wiper, the possible signal distortion, and the potentiometer life. Test results showed a clean signal output with no indications that centrifugal force was affecting the nylon line, and sufficient life to complete the planned tests.

Wing Spar. During wind tunnel testing the wing was to be subjected to beamwise and chordwise bending and torsional displacements. Estimates were made as to the likely wing tip deflections in each axis. These were:

Beam	20 mm/5g*	* whichever was less, at a given frequency.
Chord	10 mm/5g*	
Torsion	1.5°	

As a conservative approach, it was assumed they would be at a maximum together. However, little data existed to verify by calculation that the spar had an adequate fatigue life in combined bending and torsion and therefore substantiation testing was carried out.

The wing spar was cantilever mounted with the rectangular box section orientated such that the required ratio of beam/chord bending was achieved. A sinusoidal load off-set from the box centre to give the correct bending/torsion ratio was applied. This test also enabled the joint integrity at each end to be confirmed. Although both the composite box and metal fittings were tested to their fully factored loads separately, the inboard joint did not achieve the composite factored load levels. It was therefore decided to reduce the allowable bending deflections to:

Beam	15 mm/5g*	* whichever was less.
Chord	7.5 mm/5g*	

Drive Shaft. There was a concern as to whether the drive shaft would increase the model wing structural damping whilst transmitting torque. Beam and chord rap tests were carried out on a test wing and dummy nacelle mass and the damping determined using the log decrement method. The drive shaft was fitted, static torque applied and the rap tests repeated. Little effect was observed on beam damping but the chord damping increased to around 5% critical. This was considered acceptable as the wing/nacelle used in the wind tunnel tests would have a higher mass and stiffness. However this remained a concern through to the wind tunnel tests.

4. MODEL COMMISSIONING

Initial commissioning of the rotor head was carried out at WHL. A set of wooden blades from previous aerodynamic test work was made available and an existing model rotor rig used for the tests. An analysis was conducted to ensure the rotor/blade configuration was stable and to define the test parameters. Rotor speed was chosen to match the centrifugal load of the EUROFAR model blades, at the hub spindles. The performance of the rotor head was determined up to 15° of collective pitch and 6.5° of gimbal tilt. The rotor head and associated instrumentation performed satisfactorily.

Further commissioning was carried out at Sikorsky Aircraft, Stratford, Connecticut, USA in their hover facility. The nacelle was mounted on a 'rigid' wing (used by Sikorsky for their VDTR test) throughout this stage of the commissioning. Prior to fitting the rotor head rap tests were carried out on the EUROFAR blades to determine the various blade modes. This was carried out both with the gimbal locked and free.

Initially the wooden blades used for commissioning at WHL were fitted and the test points repeated. The results compared well with those obtained from the commissioning at WHL.

The EUROFAR blades were fitted and blade and flexure gauges calibrated. The flexure flap and lag gauges were continuously monitored during the tests. All other instrumentation channels were recorded and were also on continuous display to ensure monitor limits were not exceeded. The rotor was slowly run up through the speed range. At 820 rpm the flexure edgewise strain gauge monitor limit was reached. Examination of the three flexure edgewise gauges showed this

to be an asymmetric edgewise blade mode responding at two-per-rev. It was thought the wing blockage effect and proximity of the floor was affecting the rotor wake and exciting this mode. This theory was tested by setting the nacelle to the cruise position and raising the wing away from ground (a hydraulic ram formed the base of the test stand). Testing in this configuration showed a substantial reduction in the blade edgewise vibration and allowed the rotor to be run up to its full operating speed in a cautious and progressive manner. For subsequent tests in the hover (with the ram lowered) the rotor speed was rapidly increased from 800 rpm to 900 rpm. Provided this was done the edgewise vibration remained within the alarm limits. The rotor performance was determined for thrusts from 0N to 580N and gimbal tilt angles up to 6.5°.

The next phase of the commissioning was carried out in the UTRC wind tunnel at Hartford, Connecticut using the flexible wing. Initially shake tests were carried out on the nacelle and flexible wing using a dummy rotor mass in place of the model rotor. (Figure 5) From the resulting transfer functions modal damping and inertias were calculated and used to improve the stability predictions for the cruise conditions.

The rotor head and blades were re-assembled to the nacelle. The same parameters were recorded as in previous tests. In addition both wing beam and chord accelerations, and the outputs from six accelerometers mounted on the transmission were recorded. The model performance was determined through the nacelle tilt range of 0-90° at zero wind speed. (Figure 6) A small amount of gimbal tilt (1.5°) was also applied. For high thrusts and nacelle tilt angles above 60° the wind tunnel walls were affecting the rotor inflow and wake. The model was therefore yawed 30° approx on the tunnel balance and high thrust conditions completed. Commissioning of the rotor excitation system was carried out to identify the wing and blade modes, and the direction and level of forcing necessary to excite each mode. As each mode was identified a recording of all instrumentation outputs was taken. Approximately one second after recording started the excitation system was turned off. Specific channels were subsequently analysed using a moving block analysis program to determine damping levels.

A wing flutter test was carried out as a safety check, taking the nacelle and flexible wing to the maximum tunnel speed of 84 m/s. An eccentric mass was used to excite the wing. This replaced the rotor head assembly but had the same mass and is shown in Figure 5. It served as a shaker to excite the wing modes by using out-of-balance forces whilst being rotated on the rotor shaft. Moving block analysis was carried out at the mode frequency on data obtained as the eccentric mass was moved rapidly off resonant speed. The initial tests were carried out with the stiffest torsion bar fitted. The tests were repeated with a soft torsion bar which showed that there was significant friction in the pitch mechanism. Damping was greater for the soft bar than with the stiff bar, with no significant change in frequencies.

5. THE WIND TUNNEL TEST

The wind tunnel test running was conducted over a period of 4 days (25 to 28 January 1993). The principal objective was to obtain data to define the stability margins and boundaries in the cruise configuration (zero nacelle tilt). A secondary objective was to obtain loads and trim data, most importantly in conversion configurations (intermediate nacelle tilts, see Figure 6), but also in cruise.

Limitations to the originally planned variation of model parameters for the test were driven by technical and schedule considerations. Technically, the interchangeable torsion bars in the tilt mechanism had been identified as largely ineffective in commissioning tests, due to friction. To minimise damping, the datum configuration chosen for the wind tunnel tests was therefore a stiff steel bar. A high priority was attached to testing the rotor configuration of 20° δ_3, since this was predicted as the least stable, and hence most likely to give the clearest validation data.

For the cruise conditions (ie. nacelle at zero tilt, rotor shaft parallel to the wind axis), the following five configurations were successfully tested:

Rotor Speed (rpm)	Thrust (nominal, N)	Delta3 (degrees)	Torsion Bar
900	0 and 67	0 and 20	stiff
1124	0	0	stiff

Thrust values for the conditions tested are given as "nominal", since unresolved problems in accurate measurement of thrust (from the sum of rotor balance and pitch link loads) led to the use of measured rotor torque to set the conditions. An assumption of 80% cruise efficiency was used to define a target torque corresponding to the nominal 67N cruise thrust, while zero torque was used for the nominal zero thrust points (or, in hover, minimum torque). When the model was on condition at a cruise test point, a steady-state data record was taken (for loads and trim data). The swashplate excitation system was used to excite each wing mode in turn (using longitudinal cyclic input for the beam and torsion modes, collective input for the chord mode). Some assessment was also made of the blade lead-lag mode (using cyclic input). This was very lightly damped in the hover but acquired high levels of damping as airspeed was increased, such that excitation of this mode was curtailed. The damping of each mode was analysed using the moving block program. Beamwise and chordwise wing motions were derived from the corresponding wing-tip accelerometers. Torsion was derived from the chordwise accelerometer. Flexure bending gauges were used to evaluate blade motions.

For conversion test points (non-zero nacelle tilts), a steady-state data record was taken, for loads and trim data, and only the 20° δ_3 configuration was tested.

5.1. Prediction Methods

The primary objective of the tests was the validation of prediction methods for tilt-rotor aeroelastic stability, principally with reference to whirl-flutter. The WHL Coupled Stability Analysis (CSA) was configured as such a method for the EUROFAR Project.

In CSA the rotor is described by mode shapes and natural frequencies of the rotating cantilevered blade, superimposed on a gimbal model which in turn is configured on an aircraft structural model described by its modes. The gimbal model includes structural stiffness and damping, with undersling and pitch-tilt coupling (δ_3) geometry. Quasi-static aerodynamics are used for the blade, with distributed aerofoil sections described by lift, drag and pitching moment coefficients against angle of attack and Mach number. No wing

aerodynamics are included. Structural damping is input in modal form for the blades and aircraft structure. This was input to match the beam mode 0m/s measured value (at 900 rpm, 0° δ_3) with an assumption of 3% damping in the chord and torsion modes and 0.5% for the blade modes.

Fundamental modes of the cantilevered rotating blade were calculated using the WHL blade modes program (J134). This dynamic model exhibited good agreement with the non-rotating blade rap test results. A single set of blade modes was used in CSA for each cruise configuration, calculated at the trim point of the corresponding highest measured test velocity. For each velocity, the rotor was re-trimmed to the measured power, in CSA with the blade modes unchanged. Multiple sets of modes may be used, but in practice the change in rotor dynamics over the velocity range of interest, close to the stability boundary, may be considered small.

The structure modes for the model were obtained from a NASTRAN finite element representation of the test stand, wing and nacelle, with the rotor mass included. The test stand and wing were modelled principally by beam elements, with some use of rigid bars and springs. A simplified nacelle model was used, based on rigid bars and concentrated masses, with a spring element for tilt-mechanism stiffness. A transmission representation was included, primarily to evaluate the significance of transmission dynamics, including shaft whirl, prior to the tests. For the structure representation in CSA, the fundamental wing modes were used (beamwise, chordwise and torsion), with the rigid-body transmission mode. Nacelle mass, inertia and centre of mass, initially estimated, were taken from measurements recorded during the commissioning. Shake test results for the model were obtained during commissioning, allowing comparisons with the theoretical model and some fine-tuning.

5.2. Discussion of Results

The results presented are from initial analysis of data records. Comparisons are made with preliminary predictions of stability.

Aeroelastic Stability in Cruise. Results are shown in Figures 7-9 for damping of the wing beam, chord and torsion modes against velocity, for the 900 rpm 0° δ_3 configuration. Values for both zero and non-zero torque conditions are plotted as points, with corresponding predictions plotted as solid and dashed lines, respectively. For the beam mode (Figure 7), damping rises with velocity from 0.7% at 0m/s to a peak around 3.0% at 60 m/s (zero torque case) before falling steeply to 0 at 68.6 m/s. As the stability boundary was approached, with tunnel speed slowly increased, the beam mode motion appeared spontaneously, initially fluctuating in amplitude at low levels, then in a sustained manner, growing in amplitude. Wind tunnel speed was decreased to fallback condition as rapidly as possible, with simultaneous control of blade pitch and rotor speed to maintain acceptable trim. The boundary speed value was obtained by visual assessment of wing motion. The non-zero torque conditions exhibit a lower level of damping above 45 m/s than those at zero torque, although the stability boundary point is the same. The predictions for the beam mode agree well with measurement, with a small over-estimate of the boundary speed and a somewhat less steep damping rise and fall prior to the boundary. The de-stabilising effect of torque is shown, right up to the boundary.

Chord mode damping (Figure 8) shows an increase as the beam stability boundary is approached (at least at zero torque), remaining above 2.5% throughout the velocity range. There is considerable scatter in results at high speed, where high levels of blade lead-lag motion in the mode restricted the level of allowable excitation seen at the wing accelerometer. Some conditions were re-analysed using blade strain gauge data. When transposed into the fixed frame of reference, these results cast doubt on the 2 high-damping results (above 14%). At such high damping the accuracy of the moving block method is in any case open to question. The zero torque cases are below the non-zero torque damping for much of the speed range, with exception of a single point above 60 m/s and the zero velocity point (possibly due to scatter). The predictions reflect the trend in measured damping well but tend to over-estimate it at higher speeds.

Considerable scatter in torsion mode damping (Figure 9) masks any trend with increasing velocity. The minimum measured damping, at just over 2%, is not reflected in the prediction. The chordwise wing tip accelerometer used was increasingly restricted in amplitude at higher speeds due to high blade lead-lag motion in the excited torsion mode. A requirement to re-analyse the data using blade gauge output has been identified, in order to improve accuracy.

Frequency measurements (Figure 10) show the wing beam mode results closely reflected by prediction. The chord mode frequency remains substantially constant with the theoretical result indicating a fall in frequency with increased velocity. The torsion frequency reduction with velocity is under-predicted, with 6.7 Hz predicted at high speed. Despite the use of a stiff torsion bar in the tilt mechanism, evidence shows that the wing torsion frequency fell by around 0.5 Hz between commissioning trials and the wind tunnel test, following re-work to free the tilt mechanism bearings. During the test motion was detected in the tilt angle measurement potentiometer. The source of nacelle flexibility, most probably in the tilt mechanism, is approximated by a discrete spring between the nacelle and the wing tip in the current structural model. Some evidence of reducing torsion frequency with velocity was seen in the wing flutter check (without the rotor), implying a requirement for wing aerodynamics to be included in the prediction method for the complete model.

Results for measured damping in the wing beam mode at 1124 rpm and zero torque are shown in Figure 11. Although less data were recorded for this rotor configuration, and the stability boundary was not defined, the trend clearly indicates a peak in damping around 53 m/s. The effect of increased rotor speed is to flatten the peak, with a less steep decline in damping, which is reflected by the prediction.

Figure 12 shows the beam mode damping for the 900 rpm 20° δ_3 configuration. The de-stabilising effect of the δ_3 coupling is very apparent (compared with Figure 7), with a reduction in boundary velocity of around 9 m/s (13%), together with steeper damping rise and fall. The prediction reflects this trend well, together with the destabilising effect of non-zero torque, but under-predicts the boundary speed.

Conversion Conditions. A total of 16 conditions were achieved, defined from trim predictions for the full scale aircraft. A deviation from the planned test programme was the exclusive use of the 20° δ_3 rotor geometry. This was retained following stability tests to optimise use of available wind tunnel time. As with the cruise tests, the rotor was trimmed to torque rather than thrust. For some points, blade

collective pitch was increased until a monitor limit was reached (usually rotor torque) before data was taken. All points were at a target rotor speed of 1124 rpm.

The achieved test points are plotted on Figure 13, as nacelle tilt against wind speed. Three points are defined as the high speed conversion corridor boundary points, obtained at the highest attempted speed at each nacelle tilt used (30°, 60° and 80°). The boundary points are shown joined by a dashed line, which represents the corridor boundary successfully demonstrated by the tests. At all points gimbal tilt was successfully trimmed out. Available cyclic pitch limits were approached on 1 point, with a resultant measured value of 10 degrees. On several occasions during the test, the nacelle tilt angle was changed at non-zero wind speed (up to 32 m/s), over the range of 80 degrees to zero (cruise). No adverse loading or controllability was experienced.

Loads and trim data were recorded at each conversion point, thus establishing a database for future comparison with predicted data as a basis for validation of prediction methods.

6. CONCLUSIONS

The EUROFAR aeroelastic stability wind tunnel model (Model 3) has been successfully designed, substantiated, commissioned and tested, obtaining valuable data defining aeroelastic (whirl-flutter) stability boundaries and margins in cruise flight, and loads and trim data in cruise and conversion regimes.

These data contribute to the EUROFAR tilt rotor technical database and provide a basis for validation of aeroelastic stability and loads prediction methods.

The tests achieved the successful demonstration and recording of stability margins and boundaries for 5 different rotor configurations, encompassing variations in rotor speed, thrust levels and gimbal δ_3 coupling (effective blade pitch-flap coupling).

A positive δ_3 of 20° was found to be strongly destablising as prediction had indicated. Stability margins were found to be relatively insensitive to thrust levels. Increased rotor speed decreased margins, at least below the stability boundary speed.

Sixteen conditions in the conversion regime were evaluated, with loads and trim data recorded. High speed boundary points on the conversion corridor were reached. Full scale equivalent air speeds were 125 knots at 80° nacelle flight, 168 knots at 60° and 172 knots at 30° (where zero tilt is cruise).

Strategic use of model substantiation and commissioning activity resulted in these achievements being possible within rigorous time-constraints of a single test period in the wind tunnel.

Initial predictions for aeroelastic stability show good agreement with measured trends, with deviation from absolute values in some cases.

7. FURTHER WORK

Further detailed analysis of the results will be carried out. To improve the quality of the damping results it is intended to repeat

the moving block analysis of the wing modes using the blade flexure gauges.

Further investigation to improve theoretical modelling will proceed, including consideration of wing aerodynamics and a more detailed structural model of the nacelle, reflecting in particular the load paths and flexibilities in the tilting degree of freedom. Rotor loads calculations will be compared with measurements in the conversion mode.

The model has the potential for further testing to investigate the effects of tilt mechanism stiffness, gimbal stiffness and negative δ_3 coupling. To assess the effect of varying the tilt mechanism stiffness some modifications to the model are necessary. This would primarily be replacing the transmission trunnion Oilite bearings with antifriction bearings.

8. ACKNOWLEDGEMENTS

The authors express their gratitude to the many people who contributed to this project; to numerous colleagues at WHL and those at Sikorsky Aircraft (in particular Gordon Miller and Tony Saccullo) and UTRC. EUROFAR is part-funded by the UK Department of Trade and Industry and is a EUREKA project.

9. REFERENCES

1 Juggins P T W et al, "Experimental Activities to Support the EUROFAR Tilt Rotor Project Preliminary Phase", Presented at the Royal Aeronautical Society EUROFAR One Day Conference, London, 11 April 1989.

2 Beroul F, Bassez P and Gardarein P "EUROFAR Rotor Aerodynamic Tests", Paper No. 127, presented at the 18th European Rotorcraft Forum, Avignon, September 1992.

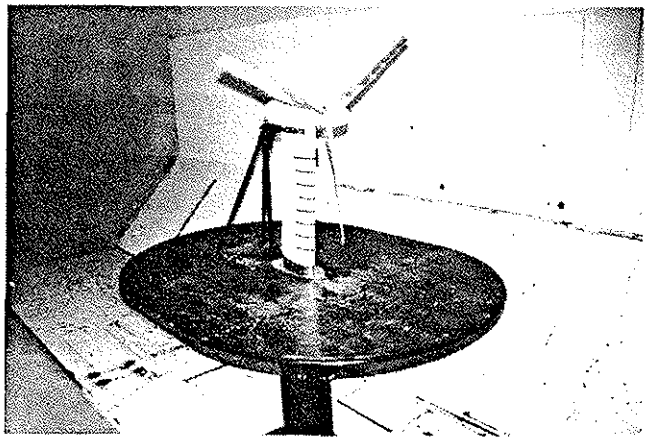

Figure 1

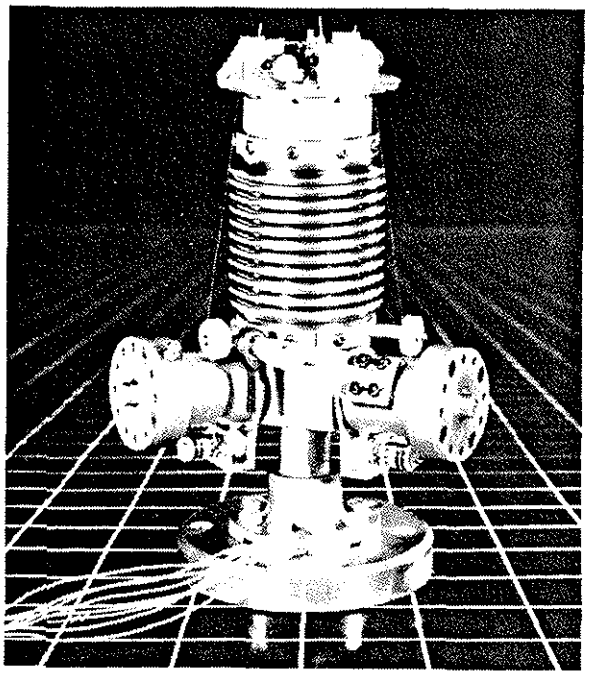

Figure 2

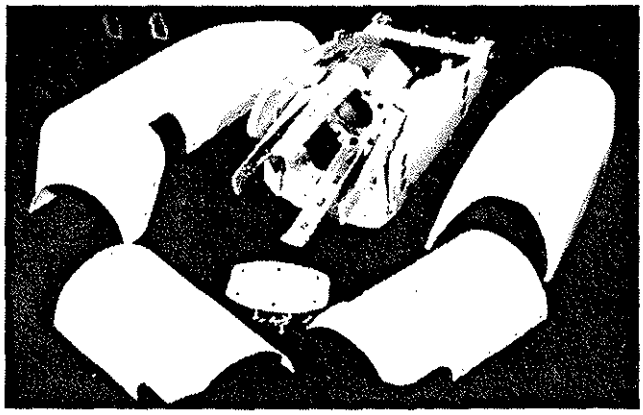

Figure 3

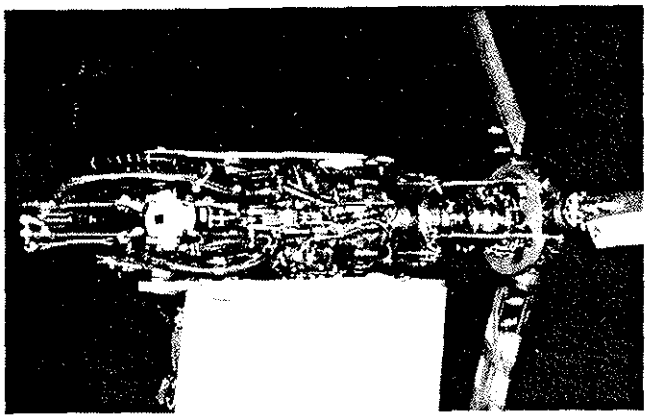

Figure 4

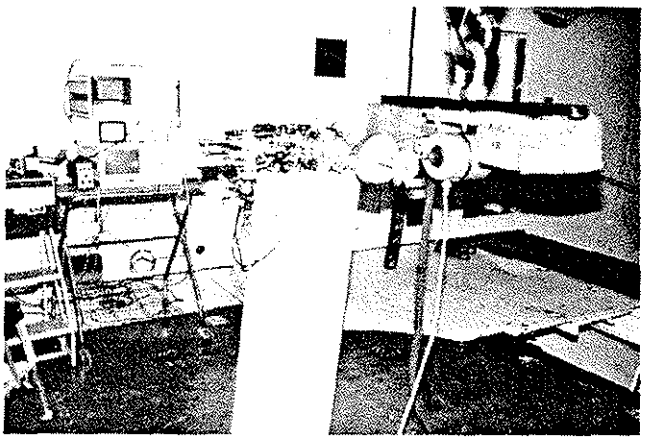

Figure 5

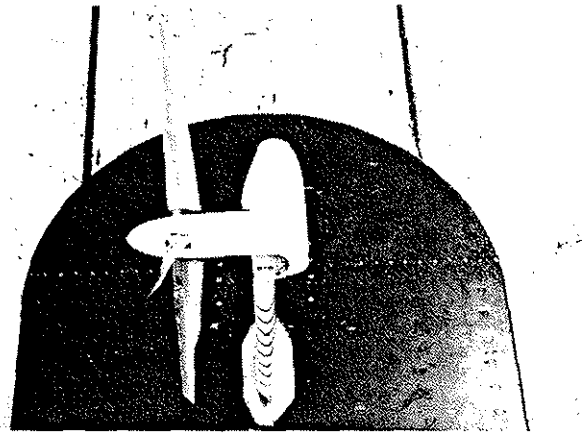

Figure 6

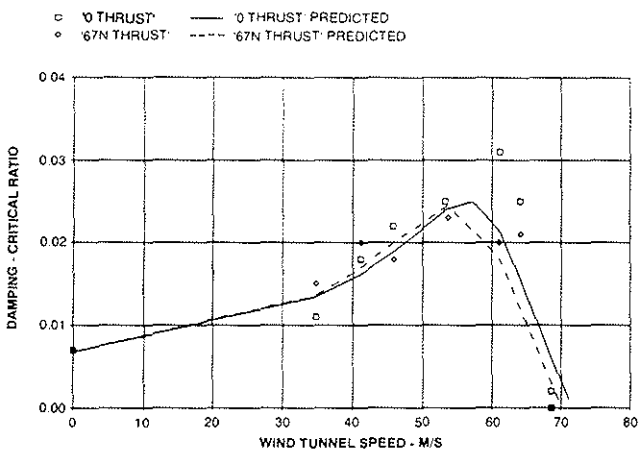

Figure 7 WING BEAM MODE DAMPING
ROTOR SPEED 900RPM $0°\delta_3$

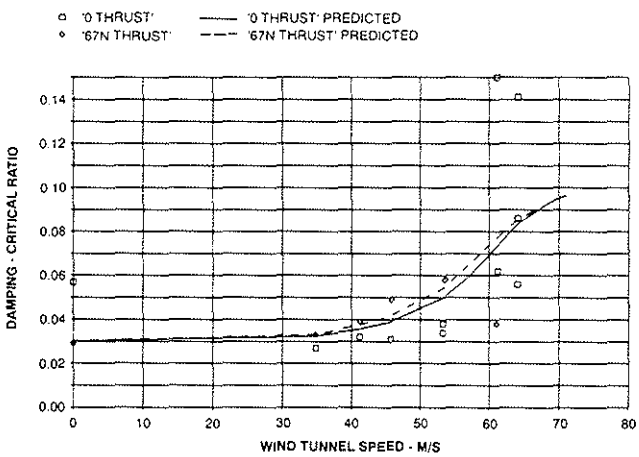

Figure 8 WING CHORD MODE DAMPING
ROTOR SPEED 900RPM $0°\delta_3$

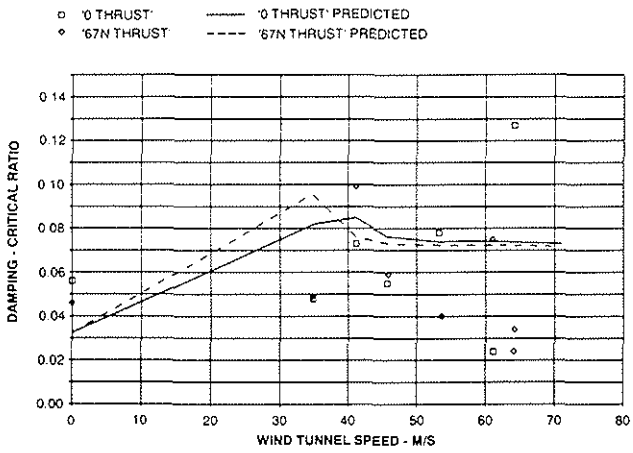

Figure 9 WING TORSION MODE DAMPING
ROTOR SPEED 900RPM 0°δ_3

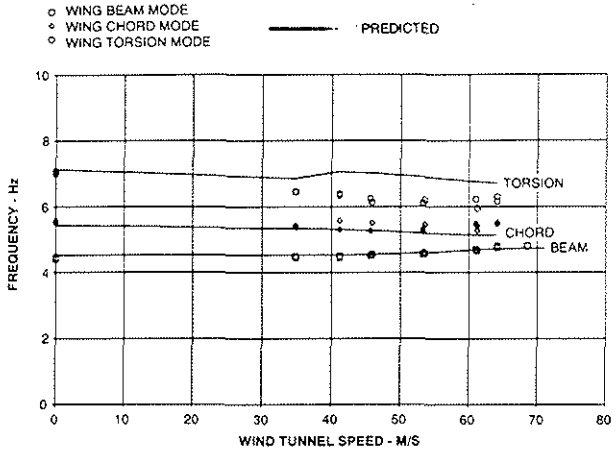

Figure 10 WING FREQUENCIES
ROTOR SPEED 900 RPM 0°δ_3

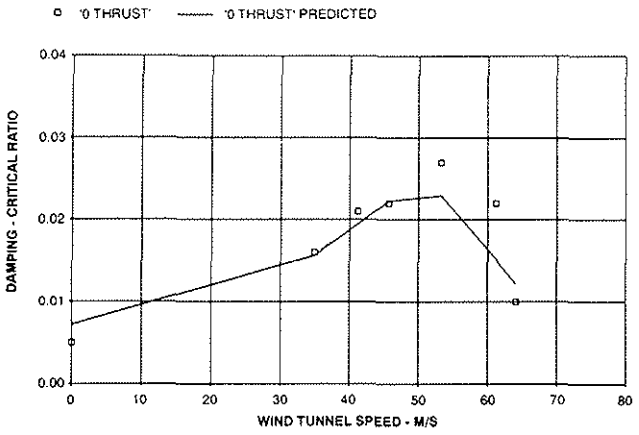

Figure 11 WING BEAM MODE DAMPING
ROTOR SPEED 1124 RPM 0°δ_3

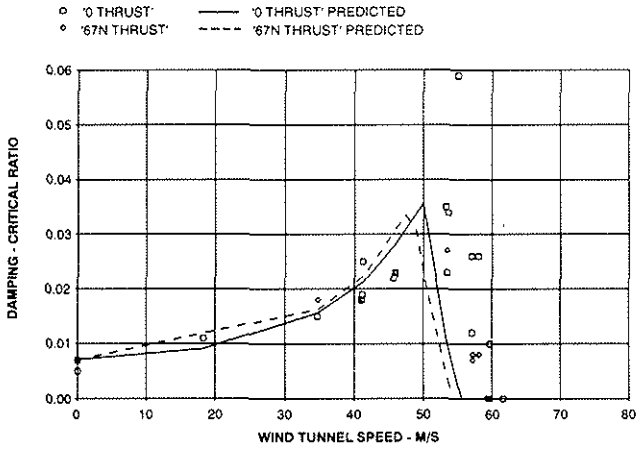

Figure 12 WING BEAM MODE DAMPING
ROTOR SPEED 900 RPM 20°δ_3

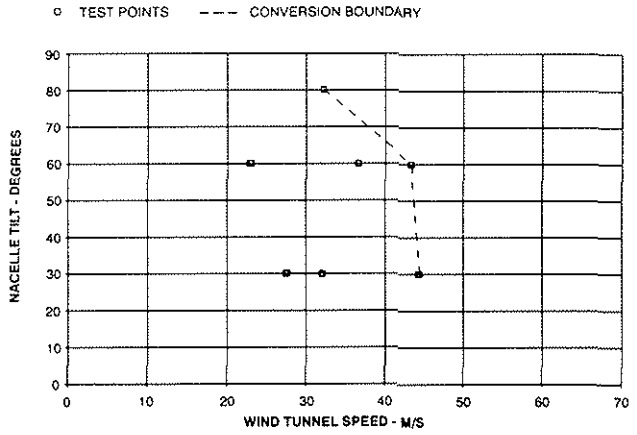

Figure 13 CONVERSION NACELLE TILT v. AIRSPEED
ROTOR SPEED 1124 RPM 20°δ_3